

Cosmological parameter estimation and Bayesian model comparison using VSA data

Anže Slosar¹, Pedro Carreira², Kieran Cleary², Rod D. Davies², Richard J. Davis², Clive Dickinson², Ricardo Genova-Santos³, Keith Grainge¹, Carlos M. Gutiérrez³, Yaser A. Hafez², Michael P. Hobson¹, Michael E. Jones¹, Rüdiger Kneissl¹, Katy Lancaster¹, Anthony Lasenby¹, J. P. Leahy², Klaus Maisinger¹, Phil J. Marshall¹, Guy G. Pooley¹, Rafael Rebolo^{3,4}, José Alberto Rubiño-Martin^{3,‡}, Ben Rusholme^{1,*}, Richard D. E. Saunders¹, Richard Savage¹, Paul F. Scott¹, Pedro J. Sosa Molina³, Angela C. Taylor¹, David Titterton¹, Elizabeth Waldram¹, Robert A. Watson^{2,†} and Althea Wilkinson².

¹ *Astrophysics Group, Cavendish Laboratory, Madingley Road, Cambridge CB3 0HE, UK.*

² *Jodrell Bank Observatory, Macclesfield, Cheshire SK11 9DL, UK.*

³ *Instituto de Astrofísica de Canarias, 38200 La Laguna, Tenerife, Spain.*

⁴ *Consejo Superior de Investigaciones Científicas, Spain*

[†] *Present address: Instituto de Astrofísica de Canarias.*

^{*} *Present address: Stanford University, Palo Alto, CA, USA*

[‡] *Present address: Max-Planck Institut für Astrophysik, Garching, Germany*

Accepted —; received —; in original form 14 March 2019

ABSTRACT

We constrain the basic cosmological parameters using the first observations by the Very Small Array (VSA) in its extended configuration, together with existing cosmic microwave background data and other cosmological observations. We estimate cosmological parameters for four different models of increasing complexity. In each case, careful consideration is given to implied priors and the Bayesian evidence is calculated in order to perform model selection. We find that the data are most convincingly explained by a simple flat Λ CDM cosmology without tensor modes. In this case, combining just the VSA and COBE data sets yields the 68 per cent confidence intervals $\Omega_b h^2 = 0.034_{-0.007}^{+0.007}$, $\Omega_{\text{dm}} h^2 = 0.18_{-0.04}^{+0.06}$, $h = 0.72_{-0.13}^{+0.15}$, $n_s = 1.07_{-0.06}^{+0.06}$ and $\sigma_8 = 1.17_{-0.20}^{+0.25}$. The most general model considered includes spatial curvature, tensor modes, massive neutrinos and a parameterised equation of state for the dark energy. In this case, by combining all recent cosmological data, we find, in particular, 95 per cent limit on the tensor-to-scalar ratio $R < 0.63$ and on the fraction of massive neutrinos $f_\nu < 0.11$; we also obtain the 68 per cent confidence interval $w = -1.06_{-0.25}^{+0.20}$ on the equation of state of dark energy.

Key words: cosmology; observations – cosmic microwave background

1 INTRODUCTION

In the past two years, a number of experiments have produced accurate measurements of the power spectrum of anisotropies in the cosmic microwave background (CMB) radiation on a range of angular scales (Hanany et al. 2002; Netterfield et al. 2002; Halverson et al. 2002; Sievers et al. 2002; Benoit et al. 2002). These data, together with other cosmological observations, have been used to place increasingly tight constraints on the values of cosmological param-

eters in current models of the formation and evolution of structure in the Universe.

In this letter, we repeat this process with the inclusion of the latest observations from the Very Small Array (VSA) in its extended configuration. Results from the VSA in its compact configuration have already been presented in Watson et al. (2002), Taylor et al. (2002), Scott et al. (2002) and Rubiño-Martin et al. (2002) (hereafter Papers I - IV). In Grainge et al. (2002, hereafter Paper V) these data are combined with the new extended configuration ob-

Table 1. The priors assumed for the basic parameters common to all four cosmological models under consideration. The notation (a, b) for parameter x denotes a top-hat prior in the range $a < x < b$

Basic parameter	Prior
ω_b	(0.005, 0.80)
ω_{dm}	(0.01, 0.9)
h	(0.4, 1.0)
n_s	(0.5, 1.5)
z_{re}	(4, 20)
$10^{10}A_s$	(0, 100)

servations to produce a combined power spectrum with 16 spectral bins spanning the range $\ell = 160 - 1400$. This joint set of observed band-powers provides powerful new constraints on cosmological parameters. In this letter we extend the traditional likelihood approach of previous analyses to a fully Bayesian treatment, including careful consideration of our knowledge of cosmological parameters prior to the inclusion of any data, and the calculation of Bayesian evidences to perform model comparisons.

2 MODELS, METHODS AND PRIORS

We restrict our attention to cosmological models in which the initial density fluctuations are adiabatic with a simple power-law spectrum; such perturbations are naturally produced in the standard single-field inflationary model. We assume the contents of the Universe to consist of three components: baryonic matter, dark matter and vacuum energy, with (present day) densities denoted by Ω_b , Ω_{dm} and Ω_Λ respectively, measured as a fraction of the critical density required to make the Universe spatially-flat (with $\Omega_b + \Omega_{dm} + \Omega_\Lambda = \Omega_{tot}$).

2.1 Model parameterisation and priors

The parameterisation of the cosmological model can be performed in numerous ways, although it is generally preferable to use physically-motivated parameters along principal degeneracy directions. To this end, in the most general case, we describe the cosmological model using the following 11 parameters: the Hubble parameter h (defined as $H_0 = h \times 100 \text{ km s}^{-1} \text{ Mpc}^{-1}$); the physical baryon density $\omega_b \equiv \Omega_b h^2$; the physical dark matter density $\omega_{dm} \equiv \Omega_{dm} h^2$; the curvature density $\Omega_k = 1 - \Omega_{tot}$; the fraction f_v of dark matter in the form of massive neutrinos; the parameter w describing the equation of state of the dark energy ($p = wp$), the redshift of (instantaneous) reionisation z_{re} ; the amplitude of scalar modes A_s ; the spectral index of scalar modes n_s ; the amplitude ratio R of tensor to scalar modes and the spectral index of the tensor modes n_t .

We consider four separate models of increasing complexity, in which a successively larger number of the above parameters are allowed to vary. Model A assumes spatial flatness, no massive neutrinos and no tensor modes; Model B includes the possibility of non-zero curvature; Model C additionally allows for the presence of tensor modes; and finally Model D also allows for a contribution to the dark matter in the form of massive neutrinos and also a variable w . The variable parameters common to all four models are listed in Table 1, together with the top-hat priors assumed for each. The

Table 2. The values and priors of assumed for the basic parameters defining the four cosmological models described in the text. The notation (a, b) for parameter x denotes a top-hat prior in the range $a < x < b$.

	Model A	Model B	Model C	Model D
Ω_k	0	(-0.25, 0.25)	(-0.25, 0.25)	(-0.25, 0.25)
f_v	0	0	0	(0, 0.2)
w	-1	-1	-1	(-1.5, 0)
R	0	0	(0, 2)	(0, 2)
n_t			(-1, 0)	(-1, 0)

values and priors assumed for the other parameters are shown in Table 2 for each of the four models under consideration.

The basic parameters described above completely define the models considered. It is of interest, however, also to consider the following derived parameters: Ω_b , Ω_{dm} , $\Omega_m = \Omega_b + \Omega_{dm}$, Ω_Λ , the age of the universe, the present day rms fluctuation in $8 h^{-1} \text{ Mpc}$ spheres as predicted by linear theory σ_8 , and the optical depth to the surface of the last scattering τ . In addition to the priors listed in Table 1 and 2, we also impose the additional constraints $\Omega_\Lambda \geq 0$ and a top-hat prior on the age of the Universe lying between 10 and 20 Gyr.

2.2 Bayesian analysis using MCMC sampling

Our approach to Bayesian parameter estimation and model selection makes use of Markov-Chain Monte Carlo (MCMC) sampling to explore the posterior distribution of the cosmological parameters (see e.g. Paper IV). For any given model M , samples are drawn from the (unnormalised) posterior distribution given by the product of the likelihood and prior, i.e. $\Pr(\mathbf{d}|\theta, M)\Pr(\theta|M)$, where \mathbf{d} denotes the data under analysis and θ denotes the parameters defining the model. The likelihood function is evaluated in the same manner as discussed in Paper IV, and the joint prior is simply the product of the individual priors discussed in the previous section.

The particular implementation of the MCMC approach used is a slightly adapted version of the Cosmo-mc software package (Lewis & Bridle 2002). This sampler uses CAMB (Lewis, Challinor & Lasenby 2000) as its underlying power spectrum engine, and is specifically tailored to the analysis of CMB data. It achieves high acceptance rates and rapid convergence by using a proposal function that exploits the difference between ‘fast’ and ‘slow’ parameters in CAMB.

Given an ensemble of samples from the posterior probability distributions, we can easily obtain one-dimensional marginalised posterior distributions for any desired parameter, which thus determine the constraints implied by the data. Moreover, MCMC techniques provide a natural way to perform model selection through the evaluation of the Bayesian evidence (see e.g. Hobson, Bridle & Lahav 2002). For a given model M , the evidence is given by

$$E \equiv \Pr(\mathbf{d}|M) = \int \Pr(\mathbf{d}|\theta, M)\Pr(\theta|M)d\theta,$$

which is simply the average of the likelihood over the prior. The value of the evidence naturally incorporates the spirit of Ockham’s razor: a simpler theory, having a more compact parameter space, will generally have a larger evidence than a more complicated theory, unless the latter is significantly better at explaining the data. Thus, the problem of model selection is answered simply by identifying the model with the largest evidence. We have extended the

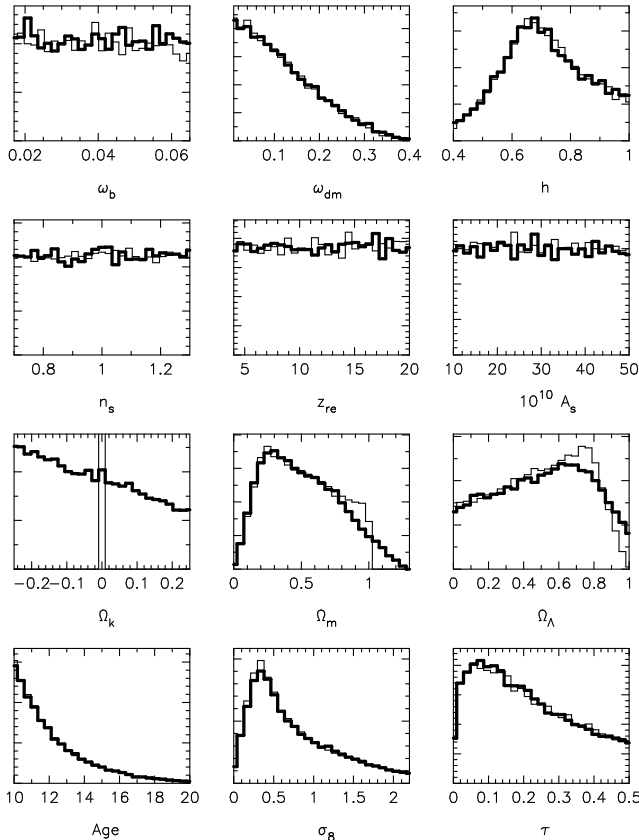


Figure 1. The one-dimensional marginalised probability distributions for cosmological parameters in Model A (thin line) and Model B (thick line) using priors alone. Thinned samples from the MCMC chains are plotted binned into histograms. The y axis shows the number of samples in arbitrary units.

Cosmo-mc program to include the calculation of the evidence by thermodynamic integration (see e.g. Hobson & McLachlan 2002). This is implemented by numerically evaluating the appropriate integral during the ‘burn-in’ of the Markov chain. ‘Burn-in’ samples are discarded for the purpose of the parameter estimation.

The resulting software was run on a 24-node Linux cluster, with each node propagating an independent chain. After burn-in, typically 5000 accepted samples were drawn from each chain, yielding a total of 120,000 accepted samples. Since successive samples from a Markov chain are, by nature, correlated, the accepted samples were thinned by a factor of 15 before analysing them further; this resulted in 8,000 independent samples. We have found that our final results are very insensitive to the thinning factor. Since each chain is run independently, we also obtained 24 separate estimates of the evidence, which are used to obtain an average value for E and an estimate of the associated error.

For calculation of confidence limits we use the 0.165, 0.5 and 0.835 points of the cumulative probability distribution. Thus, our parameter estimate is the median of the marginalised posterior pdf and the confidence interval encompasses 67% of the probability. Using the median instead of the maximum of the posterior has two advantages. Firstly, it gives consistent results under monotonic parameter transformation and combination (e.g. the median ω_b is equal to the median Ω_b multiplied by the square of the median h). This is especially advantageous in the case of cosmological parameter estimation when it is not always clear which parameters

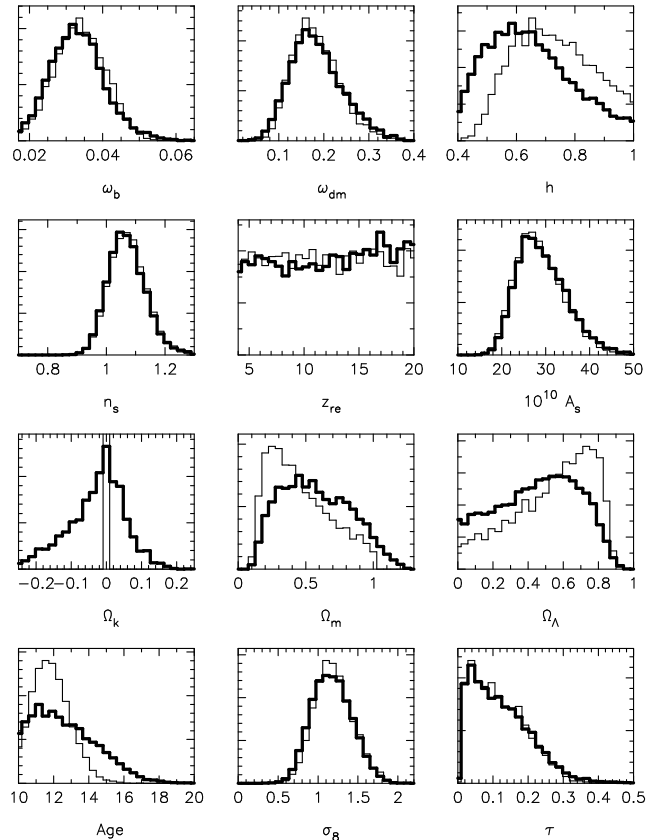


Figure 2. Marginalised posterior probability distributions of parameters from VSA and COBE data alone. The thin line corresponds to Model A and the thick line to Model B. Thinned samples from the MCMC chains are plotted binned into histograms. The y axis shows the number of samples in arbitrary units. The horizontal axes from Fig. 1 are retained.

should be considered basic (for more information see Jaynes 2002, p.621). Secondly, the method is very robust when dealing with MCMC chains: the samples may be simply sorted and searched with no need for binning and smoothing. Of course, quoting best estimates and confidence limits is simply a means of characterising the full one-dimensional marginalised distributions for each parameter. Finally, for Models A and B, the parameter estimation presented here has been repeated independently using the standard grid-based method and the results are consistent. We note that the grid based approach would be computationally prohibitive for more complex Models C and D.

2.3 Parameter constraints from priors alone

The priors on the individual basic parameters are summarised in Tables 1 and 2. As noted earlier, we also adopt the constraints (on derived parameters) $\Omega_\Lambda > 0$ and the top-hat prior (10,20) Gyr on the age of the Universe. It is of interest to determine the effect of these combined priors *alone* on the one-dimensional marginalised posteriors for each parameter. Using the MCMC sampler, this is easily performed by simply setting the likelihood to a constant value, i.e. the analysis is performed using no data. The resulting marginalised distributions for Model A and Model B are shown in Fig. 1.

These results are worthy of some discussion. Consider, for example, the distribution for h . This has a clear peak around $h \approx 0.7$, which may be understood as follows. Models with low h are rel-

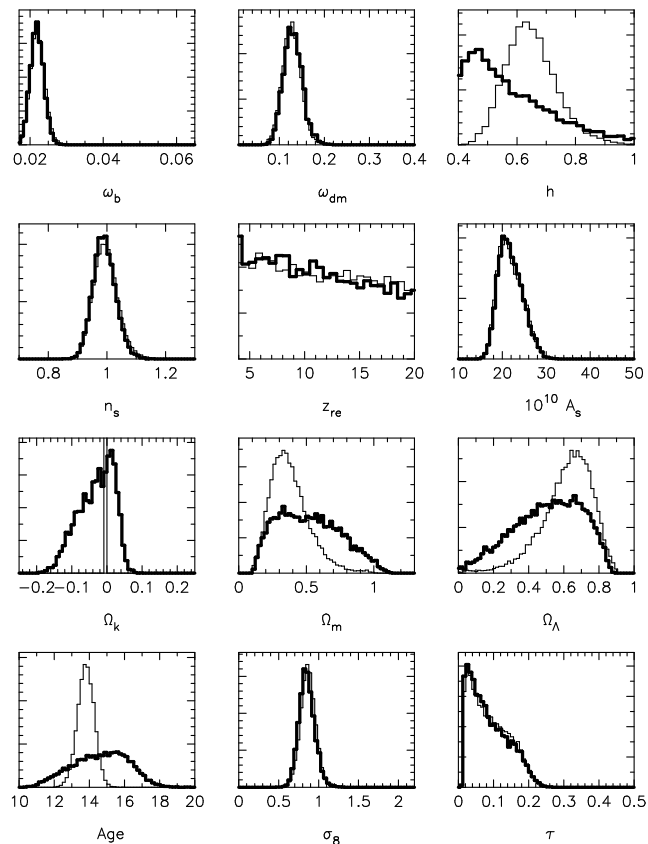


Figure 3. As for Fig. 2 but using data from all considered CMB experiments.

atively disfavoured because they would require $\Omega_\Lambda < 0$ even for modest values of $\omega_m = \omega_{\text{dm}} + \omega_b$, while models with high h are disfavoured because they tend to have ages below 10 Gyr. Similar arguments may be applied to explain the shapes of the other distributions. In particular, we note that, although broad, the distributions for Ω_m and Ω_Λ peak at 0.3 and 0.7 respectively. The non-uniformity of the distributions in Fig. 1 represents the effect of the sensible, and seemingly innocuous, initial constraints on the chosen parameters. We have also repeated the analysis for Model D, and find that the resulting marginalised distributions for the extra parameters R , n_s , f_V and w accurately follow the initial flat prior. Having made explicit the impact of our priors, we can now modulate the above distributions by including increasing amounts of data from various cosmological observations via the likelihood function.

3 RESULTS

We consider three different sets of data in our analysis. Firstly, we use only VSA data (from both extended and compact configurations using the main binning from Paper V), together with the COBE power spectrum points (Smoot et al. 1992) to constrain the low- ℓ normalisation. For this data set, we investigated just Models A and B. Secondly, we also include data from several recent CMB experiments, namely Maxima (Hanany et al. 2002), Boomerang (Netterfield et al. 2002), DASI (Halverson et al. 2002), CBI (Sievers et al. 2002) and Archeops (Benoit et al. 2002). For these data, we consider Models A, B and C. Finally, we include a wide range of additional independent cosmological probes to obtain the tightest possible constraints on the model parameters. In

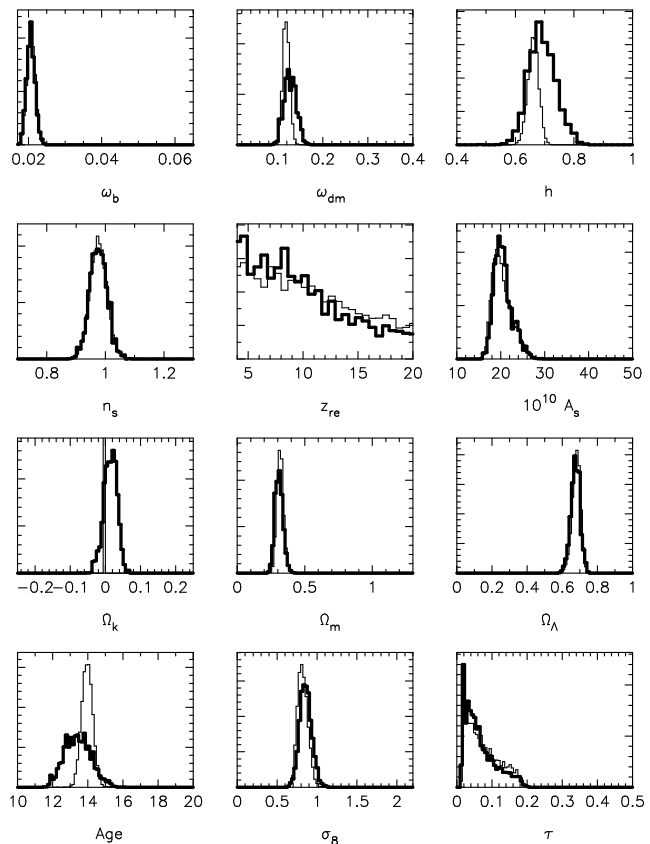


Figure 4. As for Fig. 2 but using all the data sets considered.

addition to CMB observations, we include constraints from: the HST Key Project (Freedman et al. 2001); the first 147,000 redshifts measurements from the 2dF Survey (Colles et al. 2001) on scales $0.02 < k/(h\text{Mpc}^{-1}) < 0.15$ (Lewis and Bridle 2002; Percival et al. 2002); nucleosynthesis (Burles, Nollett & Turner 2001); and type IA supernovae (Perlmutter et al. 1999). We also include the constraint from the gas fraction in relaxed clusters (Allen, Schmidt & Fabian 2002; Allen et al. 2002). We do not use the local X-ray luminosity function constraints from the cited papers due to possible systematic uncertainties. Following Allen et al., we marginalise over the cluster bias parameter. Throughout the analysis we marginalise over applicable calibration and beam uncertainty (see Paper IV).

The resulting one-dimensional marginalised posterior distributions, for each of the three data sets, are shown in Figs 2 – 4 for a selection of interesting parameters. The corresponding parameter estimates, confidence limits and evidences are given in Table 3. Note that the evidence values have been scaled so that, for each data set, Model A has an evidence E of unity.

4 DISCUSSION AND CONCLUSIONS

By comparing the effective priors on the cosmological parameters plotted in Fig. 1 with the posterior distributions inferred from the VSA and COBE data alone (Fig. 2), we see that the main strength of the VSA lies in its large ℓ -range, which allows one to constrain a wide variety of cosmological parameters. In particular, we observe that the VSA data significantly improves the constraints on ω_b , ω_{dm} , Ω_k , σ_8 and n_s . We note that, as a direct consequence of the

Table 3. Constraints on cosmological parameters; consult text for details. If a parameter is constrained, the confidence limits were obtained by calculating 0.165, 0.5 and 0.835 points of the cumulative probability distribution. When the marginalised posterior for a parameter does not contain a peak, 95% confidence limits are given. We also quote evidence values, but note that these can only be compared between models when considering the same data set.

	Model A (VSA & COBE)	Model B (VSA & COBE)	Model A (All CMB)	Model B (All CMB)	Model C (All CMB)
$\log E$	0.0 ± 0.25	-0.8 ± 0.25	0.0 ± 0.03	-1.3 ± 0.03	-3.1 ± 0.6
ω_b	$0.034 \pm_{0.007}^{0.007}$	$0.033 \pm_{0.007}^{0.007}$	$0.022 \pm_{0.002}^{0.002}$	$0.022 \pm_{0.002}^{0.002}$	$0.023 \pm_{0.002}^{0.002}$
ω_{dm}	$0.18 \pm_{0.05}^{0.04}$	$0.18 \pm_{0.05}^{0.06}$	$0.13 \pm_{0.02}^{0.02}$	$0.13 \pm_{0.02}^{0.02}$	$0.12 \pm_{0.02}^{0.02}$
h	$0.72 \pm_{0.13}^{0.15}$	$0.63 \pm_{0.13}^{0.16}$	$0.64 \pm_{0.07}^{0.09}$	$0.55 \pm_{0.10}^{0.17}$	$0.55 \pm_{0.10}^{0.17}$
n_s	$1.07 \pm_{0.06}^{0.06}$	$1.06 \pm_{0.06}^{0.06}$	$0.99 \pm_{0.04}^{0.04}$	$0.99 \pm_{0.03}^{0.04}$	$1.03 \pm_{0.05}^{0.06}$
z_{re}	unconstrained	unconstrained	unconstrained	unconstrained	unconstrained
$10^{10} A_s$	$28 \pm_4^5$	$28 \pm_4^6$	$21 \pm_2^3$	$22 \pm_2^3$	$21 \pm_2^3$
R					$0.22 \pm_{0.17}^{0.34}$
n_t					$-0.29 \pm_{0.35}^{0.20}$
Ω_k		$-0.02 \pm_{0.09}^{0.06}$		$-0.02 \pm_{0.06}^{0.04}$	$-0.04 \pm_{0.07}^{0.05}$
Ω_m	$0.42 \pm_{0.18}^{0.29}$	$0.56 \pm_{0.24}^{0.29}$	$0.36 \pm_{0.11}^{0.15}$	$0.51 \pm_{0.22}^{0.26}$	$0.46 \pm_{0.20}^{0.25}$
Ω_Λ	$0.58 \pm_{0.29}^{0.18}$	$0.47 \pm_{0.28}^{0.22}$	$0.64 \pm_{0.15}^{0.11}$	$0.52 \pm_{0.22}^{0.18}$	$0.59 \pm_{0.21}^{0.16}$
Age	$11.9 \pm_{0.9}^{1.1}$	$12.5 \pm_{1.5}^{2.1}$	$13.8 \pm_{0.4}^{0.5}$	$14.7 \pm_{1.7}^{1.4}$	$15.2 \pm_{1.8}^{1.6}$
σ_8	$1.17 \pm_{0.20}^{0.25}$	$1.16 \pm_{0.23}^{0.25}$	$0.87 \pm_{0.09}^{0.09}$	$0.85 \pm_{0.09}^{0.10}$	$0.81 \pm_{0.10}^{0.10}$
τ	$(0.01, 0.25)$	$(0.01, 0.28)$	$(0.02, 0.19)$	$(0.01, 0.19)$	$(0.02, 0.21)$
		Model A (All data)	Model B (All data)	Model C (All data)	Model D (All data)
$\log E$		0.0 ± 0.4	-2.2 ± 0.5	-3.7 ± 0.6	-6.7 ± 0.5
ω_b		$0.0210 \pm_{0.0011}^{0.0011}$	$0.0209 \pm_{0.0011}^{0.0011}$	$0.0215 \pm_{0.0011}^{0.0012}$	$0.0219 \pm_{0.0013}^{0.0014}$
ω_{dm}		$0.120 \pm_{0.007}^{0.008}$	$0.128 \pm_{0.012}^{0.014}$	$0.119 \pm_{0.014}^{0.014}$	$0.128 \pm_{0.020}^{0.020}$
h		$0.66 \pm_{0.02}^{0.05}$	$0.69 \pm_{0.04}^{0.05}$	$0.68 \pm_{0.05}^{0.05}$	$0.68 \pm_{0.05}^{0.05}$
n_s		$0.98 \pm_{0.03}^{0.03}$	$0.98 \pm_{0.03}^{0.03}$	$1.00 \pm_{0.03}^{0.04}$	$1.01 \pm_{0.04}^{0.05}$
z_{re}		$(4.00, 18.50)$	$(4.00, 18.16)$	$(4.00, 17.84)$	$(4.00, 17.95)$
$10^{10} A_s$		$20 \pm_2^3$	$20 \pm_2^2$	$20 \pm_2^2$	$20 \pm_2^2$
R				$(0.00, 0.53)$	$(0.00, 0.63)$
n_t				$(-0.88, -0.00)$	$(-0.88, -0.00)$
f_ν				$(0.00, 0.11)$	$(0.00, 0.11)$
w					$-1.06 \pm_{0.25}^{0.20}$
Ω_k			$0.02 \pm_{0.02}^{0.02}$	$0.00 \pm_{0.02}^{0.02}$	$0.01 \pm_{0.02}^{0.03}$
Ω_m		$0.32 \pm_{0.02}^{0.03}$	$0.31 \pm_{0.03}^{0.03}$	$0.30 \pm_{0.03}^{0.03}$	$0.32 \pm_{0.06}^{0.05}$
Ω_Λ		$0.68 \pm_{0.02}^{0.02}$	$0.67 \pm_{0.02}^{0.02}$	$0.69 \pm_{0.03}^{0.03}$	$0.66 \pm_{0.06}^{0.05}$
Age		$14.0 \pm_{0.3}^{0.3}$	$13.4 \pm_{0.7}^{0.8}$	$13.8 \pm_{0.8}^{0.9}$	$13.6 \pm_{0.9}^{1.0}$
σ_8		$0.82 \pm_{0.06}^{0.07}$	$0.86 \pm_{0.07}^{0.07}$	$0.83 \pm_{0.08}^{0.08}$	$0.71 \pm_{0.09}^{0.09}$
τ		$(0.02, 0.17)$	$(0.02, 0.16)$	$(0.02, 0.16)$	$(0.01, 0.16)$

pronounced third peak in the VSA power spectrum, the preferred value for ω_b is somewhat larger than that from the nucleosynthesis constraint (Burles et al. 2001) or that from the combined CMB data. This excess is statistically significant only at the 1.6σ level. VSA and COBE data alone do not, however, provide significant new constraints on either h or Ω_Λ , especially for Model B.

On comparing Figs 2 and 3, we see that, as one would expect, the constraints on all parameters are tightened by the inclusion of all the CMB data. Indeed, for Model A, reasonable constraints are obtained on all the parameters under consideration, except for z_{re} , although there is some indication that low values of z_{re} are preferred. For many of the parameters, the constraints are not significantly broader when one allows the spatial curvature to vary in Model B. Nevertheless, for this model, some parameters do become relatively unconstrained, in particular h , Ω_m and Ω_Λ , and the limits on the age of the Universe are widened considerably.

Using all recent available cosmological data sets allows one to place tight constraints on nearly all parameters, even for Model B. Indeed, only z_{re} remains relatively unconstrained, but the earlier

indication that lower values are preferred appears to be reinforced. We note that, aside from the parameters h and the age of the Universe, the constraints obtained are very similar for Model A and Model B. In fact, from Table 3, we see that, even for Models C and D, the constraints on the parameters plotted in Fig. 4 are not significantly broadened. In Fig. 5, we also plot the constraints obtained on the additional parameters R , n_t , f_ν and w for Model D. We see that the data favour low values of R and high values of n_t . More significant constraints can be placed on f_ν and w . We note from the figure that the marginalised distribution for each parameter possesses a single peak, although these are not pronounced features, especially for f_ν . Of particular interest is that the preferred value of w corresponds to a cosmological constant and that a firm upper limit is obtained on the fraction of dark matter in the form of massive neutrinos.

To distinguish between the different cosmological models considered here, we have calculated the Bayesian evidence for each model-data set combination. It must be remembered that evidence values can only be compared between different models using the

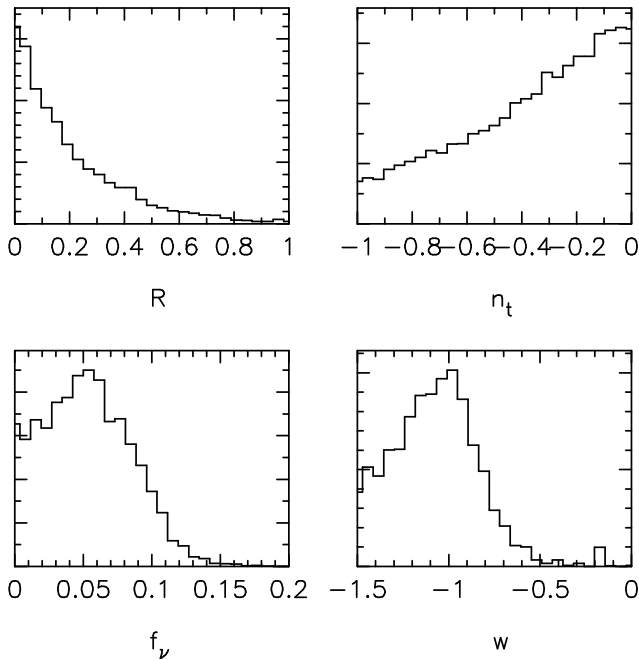


Figure 5. Marginalised posterior probability distributions of additional parameters for Model D using all data sets considered.

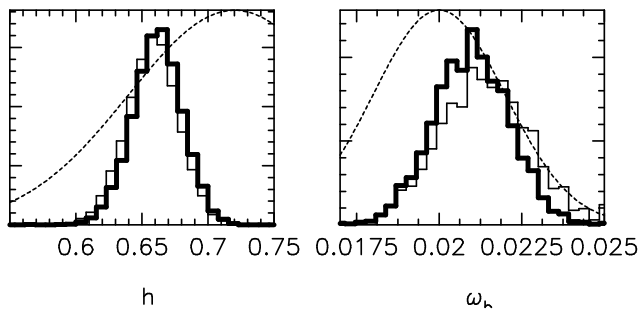


Figure 6. Marginalised posterior probability distributions for h and ω_b for Model A, using all cosmological data, with (thick line) and without (thin line) the relevant direct constraints (dashed line) from the HST Key Project and nucleosynthesis respectively.

same data set. From Table 3, we see that, for each data set, Model A (i.e. the simple 6-parameter Λ CDM cosmology) is preferred, although the evidence ratio between Model A and Model B is of order unity in each case. For Models C and D, however, the evidence ratio with Model A is considerably larger and shows clearly that such general models are not necessary to explain current cosmological observations.

Since Model A is found to have the largest evidence, it is of interest to consider more closely the impressively tight parameter constraints that can be achieved in this simple case using all the available cosmological data. In particular, let us focus on h and ω_b , which are parameters directly probed by the HST Key Project (Freedman et al. 2001) and nucleosynthesis data (Burles et al. 2001). In Fig. 6, we plot the posterior distributions of these parameters for Model A, with (thick line) and without (thin line) the corresponding direct constraint (dashed line). In each case, we see that the direct constraint is overwhelmed by the combination of the other data sets.

It is clear from the above analyses that the constraints on the

parameters in the simplest models become impressively small when a wide range of cosmological probes are used. It remains to be seen, however, whether this level of precision is matched by a corresponding level of accuracy in the values determined. The model comparison exercise demonstrated here does not address the possibility that different experiments have different systematic errors. Nevertheless, one would hope that these might be reduced when many experiments are combined. In future work, we will investigate other models, with different combinations of free and fixed parameters and perform a hyperparameter analysis (Hobson et al. 2002) to reveal any discrepancies between data sets.

ACKNOWLEDGEMENTS

We thank Antony Lewis and Sarah Bridle for providing their Cosmo-mc code and many useful discussions regarding MCMC parameter estimation. We thank Carolina Ödman for useful discussions. We also thank the staff of the Mullard Radio Astronomy Observatory, the Jodrell Bank Observatory and the Teide Observatory for invaluable assistance in the commissioning and operation of the VSA. The VSA is supported by PPARC and the IAC. RS, YH, KL, and PM acknowledge support by PPARC studentships. KC acknowledges a Marie Curie Fellowship. YH is supported by the Space Research Institute of KACST. AS acknowledges the support of St. Johns College, Cambridge. We thank Professor Jasper Wall for assistance and advice throughout the project.

REFERENCES

- Allen S., Schmidt R.W., Fabian A.C., 2002, MNRAS, L11
- Allen S., Schmidt R.W., Fabian A.C., Ebeling H., 2002, MNRAS, submitted (astro-ph/0208394)
- Benoit A. et al., 2002, A&A, submitted
- Burles S., Nollett K.M., Turner M.S., 2001, ApJ, 552, L1
- Colles M. et al, 2001, MNRAS, 328, 1039
- Freedman W.L. et al., 2001, ApJ, 553, 47
- Grainge K. et al., 2002, MNRAS, submitted
- Halverson N.W. et al., 2002, ApJ, 568, 38
- Hanany S. et al., 2002, ApJ, 545, L5
- Hobson M.P., Bridle S.L., Lahav O., 2002, MNRAS, 335, 377
- Hobson M.P., McLachlan C., 2002, MNRAS, in press (astro-ph/0204457)
- Jaynes E.T., 2002, Probability Theory: The Logic of Science. CUP, in press
- Lewis A.L., Bridle S.L., 2002, PRD, in press (astro-ph/0205436)
- Lewis A.L., Challinor A.D., Lasenby A.N., 2000, ApJ, 538, 473
- Netterfield C.B. et al., 2002, ApJ, 571, 604
- Percival W. et al., 2002, MNRAS, 337, 1068
- Perlmutter S. et al., 1999, ApJ, 517, 565
- Rubiño-Martin J.A. et al., 2002, MNRAS, submitted (astro-ph/0205367)
- Scott P.F. et al, 2002, MNRAS, in press (astro-ph/0205380)
- Sievers J.L. et al., 2002, ApJ, submitted (astro-ph/0205387)
- Smoot G.F. et al. 1992, ApJ, 396, L1
- Taylor A.C. et al., 2002, MNRAS, in press (astro-ph/0205381)
- Watson R.A. et al., 2002, MNRAS, in press (astro-ph/0205378)